Submitted to ADVANCED HEALTHCARE MATERIALS

Supporting Information

for *Adv. Healthcare Mater.*, DOI: 10.1002/adhm.201300537

Reduction in Wound Bioburden using a Silver-Loaded Dissolvable Microfilm Construct

Maggie Herron[#], Ankit Agarwal[#], Patricia R. Kierski, Diego F. Calderon, Leandro B. C. Teixeira, Michael J. Schurr, Christopher J. Murphy, Charles J. Czuprynski, Jonathan F. McAnulty*, and Nicholas L. Abbott**

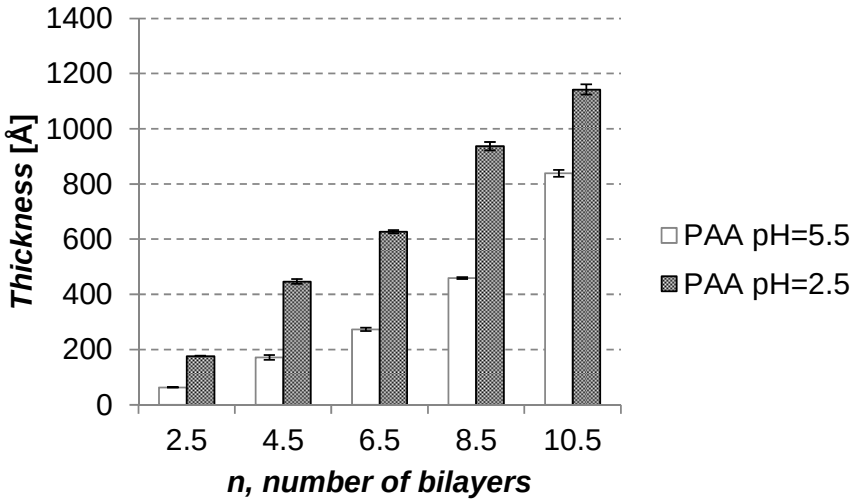

Figure S1. Ellipsometric thickness of PEMs of (FITC-PAH/PAA) with increasing number of bilayers, n, assembled on silicon wafers. Data presented as mean ± SEM with n = 12. As shown in the figure, PEMs assembled using PAA solution at pH = 2.5 are thicker than those fabricated using PAA solution at pH = 5.5. At a lower pH of PAA, there are less ionized carboxyl groups available for electrostatic binding with the charged polycations. This weaker electrostatic interaction between polymer segments, therefore, requires more polyanion deposition to compensate charge on polycations, and results in thicker multilayers. Polymer multilayers with PAA pH 2.5 shows a linear growth trend (average thickness of ~1200 Å for 10.5 bilayers), while the one with PAA pH 5.5 shows an exponential growth trend (average thickness of ~800 Å for 10.5 bilayers). This exponential growth of PEMs could be related to diffusion of single chains in and out the film in each adsorption step, causing an adsorbed amount, which is proportional to the total thickness of multilayers, yielding exponential growth.[55]

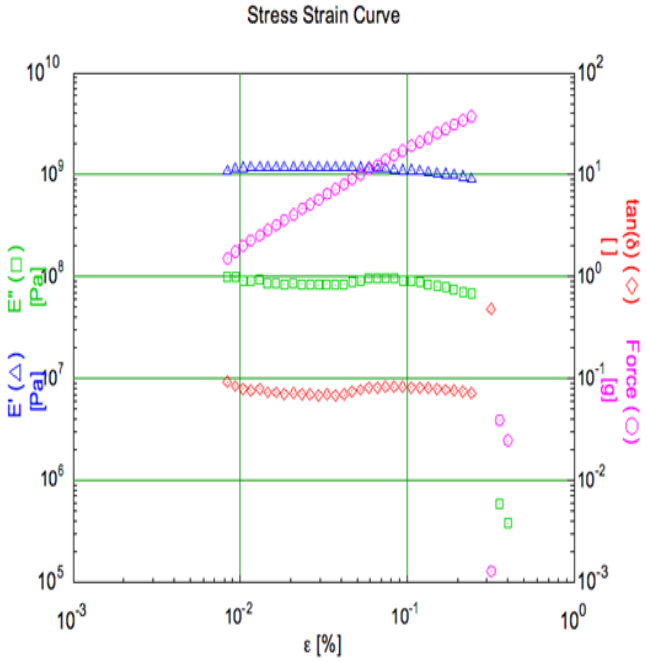

Figure S2. Mechanical strength of a PEM/PVA microfilm at 25°C in a Dynamic Strain Sweep test at 0.1 Hz frequency, as measured using a Film and Fiber tool on a Dynamic Mechanical Analyzer (DMA). Elastic storage modulus (E') was ~10^9 Pa and elastic loss modulus (E") was ~10^8 Pa. Microfilm was made of a PVA cast over PEMs of $(PAH/PAA)_{20}$ impregnated with silver-nanoparticles. Rectangular *microsheet* strips of width 3 mm were employed for this tensile testing. *Microsheet* was clamped on the tension clamp such as to provide 10 mm of specimen length.

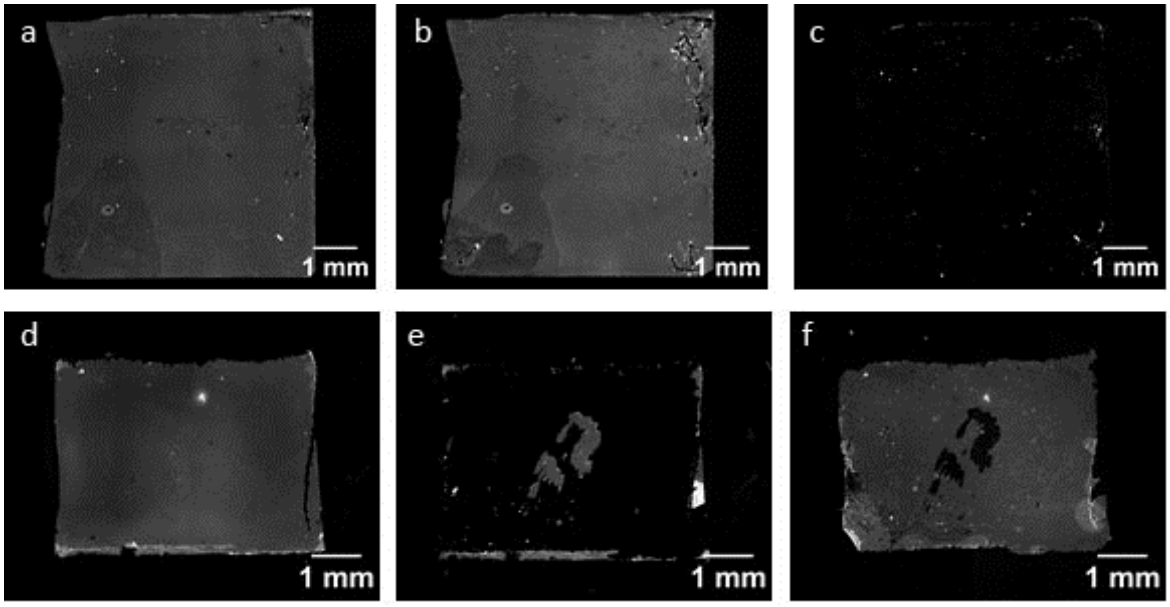

Figure S3. Fluorescent micrographs illustrate that PEMs of AF-PAH/$PAA_{5.5})_{10.5}$ (assembled using Alexa Fluor 560 labeled PAH) cannot be peeled as PEM/PVA microfilm from non OTS functionalized silicon wafer (a-c), but can be peeled uniformly from OTS functionalized silicon wafers (d-f). a,d) AF-PEMs fabricated on Si wafer substrate, b,e) PEM left on Si wafer after peeling of as PEM/PVA microfilm, c,f) PEM/PVA microfilm peeled-off the Si wafer and placed on a glass slide for imaging.

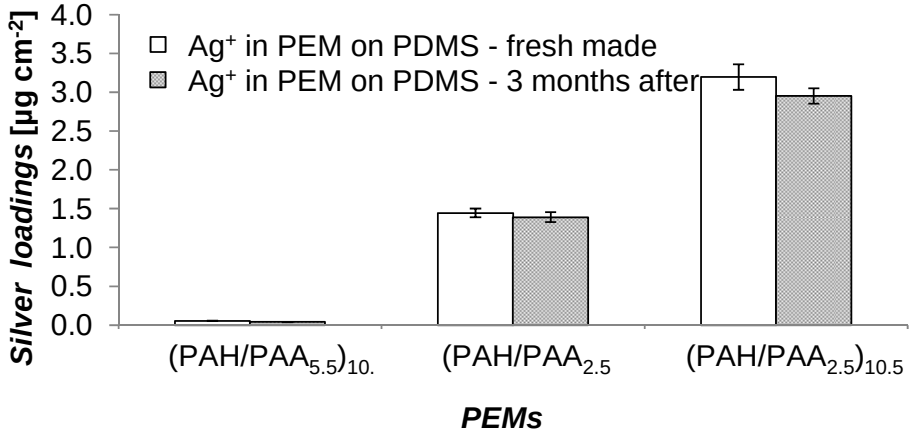

Figure S4. Silver loading in PEMs stored for 3 months at ambient temperature is not significantly different from the freshly assembled PEMs. Data presented as mean ± SEM ($n \geq 3$).

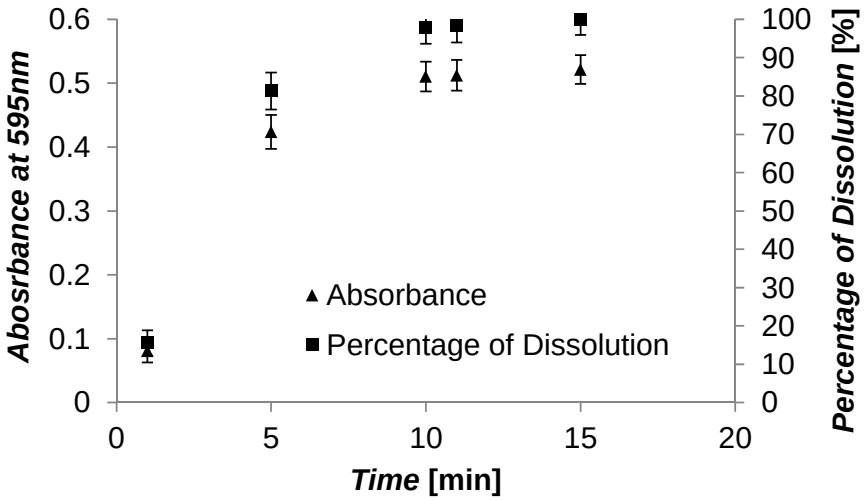

Figure S5. The PVA cast in the PEM/PVA microfilm dissolves completely in aqueous solutions within 10 min. Graph presents absorbance intensity of a Malachite Green-dye incorporated in PVA cast and released in 3 mL PBS buffer along with the dissolution of the PVA cast at different time points. Absorbance intensity of Malachite Green dye in PBS was measured on a UV-vis spectrophotometer at 595 nm wavelength. Data presented as mean ± SEM ($n \geq 5$).

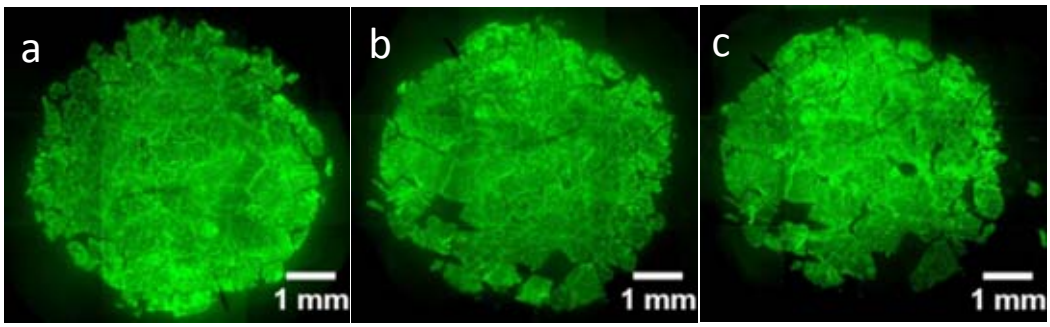

Figure S6. Fluorescent micrographs show the persistence of FITC-PEMs: (FITC-PAH/$PAA_{2.5}$)$_{40.5}$ immobilized on skin dermis against mechanical pressure and abrasion: a) FITC-PEMs immobilized on skin dermis, b) intact FITC-PEMs on skin dermis after vertically applied mechanical pressure of ~8 kPa, c) FITC-PEMs retained on skin dermis after lateral abrasion with Telfa dressings (1 mm/s) following mechanical pressure treatment described in (b).

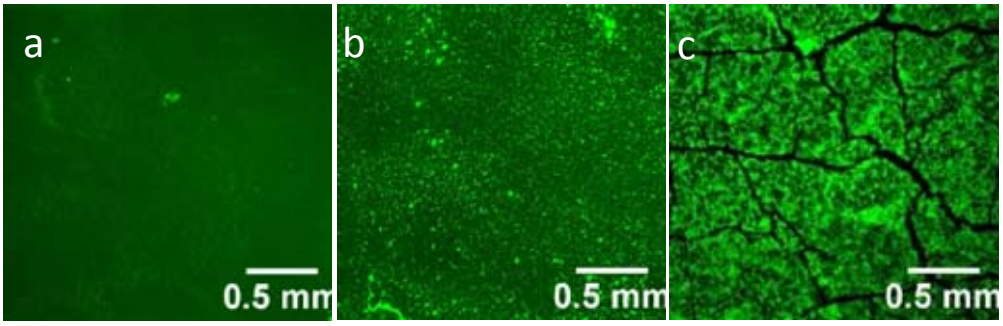

Figure S7. a-c) Formation of cracks in the PEMs of (PAH/PAA2.5) with 40.5 bilayers. Fluorescent micrographs of a) 5.5, b) 10.5, and c) 40.5 bilayers of FITC-PEMs: (FITC-PAH/PAA2.5) fabricated on elastomeric PDMS sheets**.**

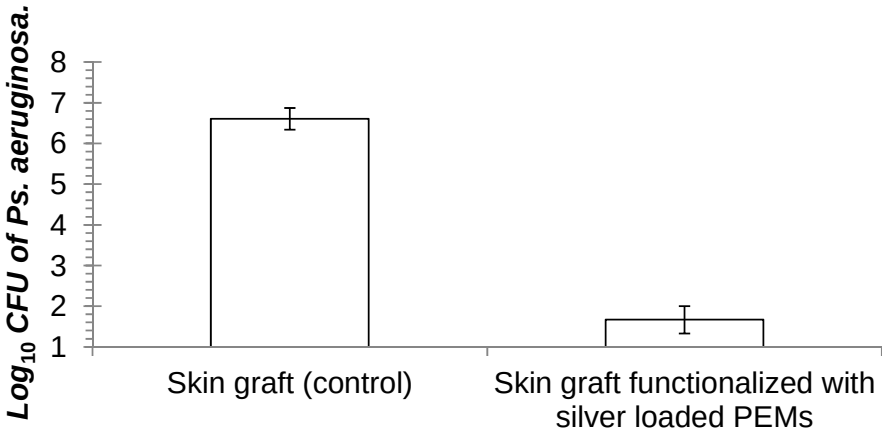

Figure S8. Antibacterial activity in suspensions of *Ps. aeruginosa* incubated for 24 h over skin-dermis modified with silver/PEMs (with silver loadings of 2.9 ± 0.1 μg cm^{-2}) using PEM/PVA microfilm. Modified skin dermis was placed in 96-well plates and incubated with 10^7 CFU of *Ps. aeruginosa* in 100 mL PBS buffer for 24 h with shaking (150 rpm) at 37°C. After incubation, bacteria were rinsed off and collected from the test wells and their serial dilutions were plated on blood agar plates. Data presented as mean ± SEM with n ≥ 4.

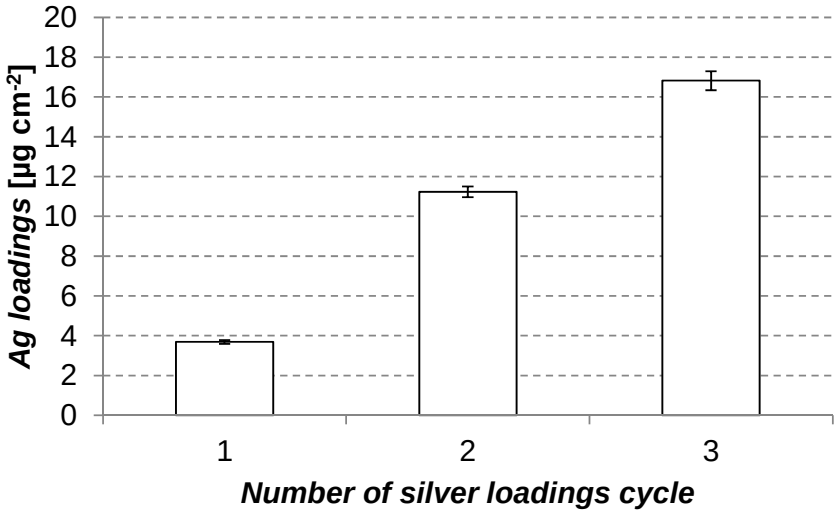

Figure S9. Silver loading in PEMs of $(PAH/PAA_{2.5})_{10.5}$ tailored up to 16.8 ± 0.5 µg cm^{-2} by repeating three cycles of silver ion exchange and their in situ reduction into silver nanoparticles. Data presented as mean ± SEM ($n \geq 4$).

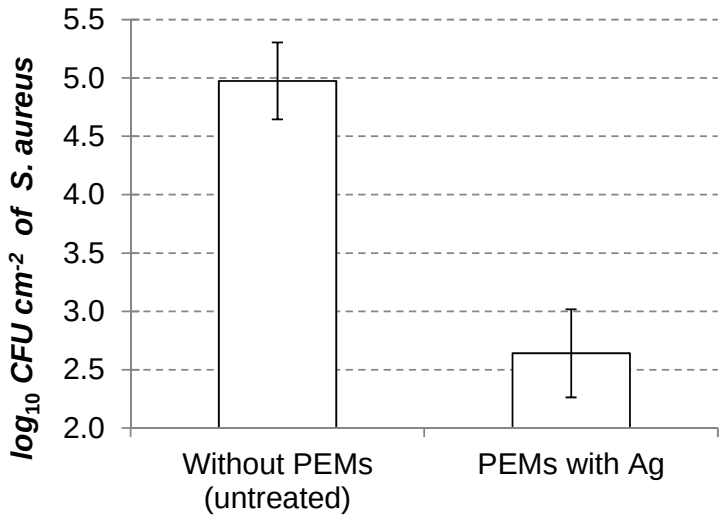

Figure S10. Inhibition of microbial colonization in contaminated murine wounds treated with PEM/PVA microfilms (with silver loading of 17.63 ± 3.13 µg cm^{-2}). Excisional 6 mm diameter splinted wounds topically inoculated with 2.71 x 10^6 CFU/cm^2 of *S. aureus* were treated with the PEM/PVA microfilm and covered with a biosynthetic wound dressing Biobrane®. Figure shows bacterial counts recovered from wounds harvested and homogenized (along with Biobrane®) after 3 days post-surgery. Data represent the mean ± SEM with n=10 mice (=20 wounds) for each group ($P < 0.001$).

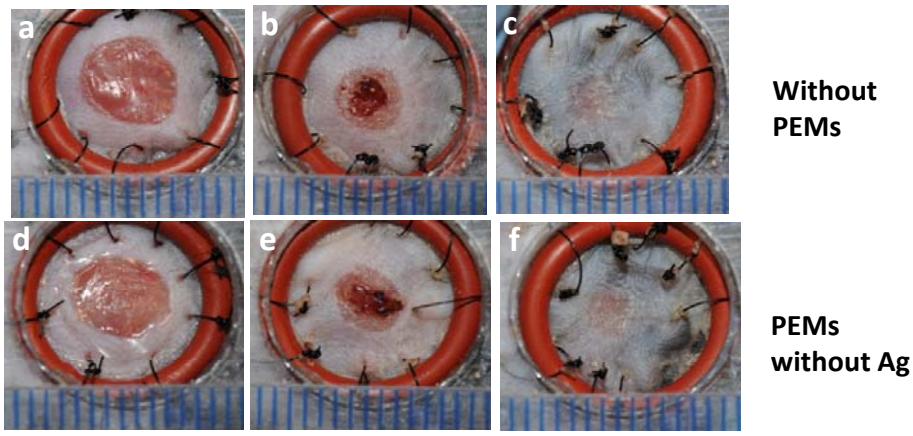

Figure S11. PEM/PVA microfilms promote normal wound healing in excisional splinted wounds in mice. Micrographs (a, b, c) show gross images of wounds without PEMs, and (d, e, f) show gross images of wounds modified with PEMs containing no silver, on post-operative days 0, 7 and 14, respectively. Each line on the scale represents 1 mm.

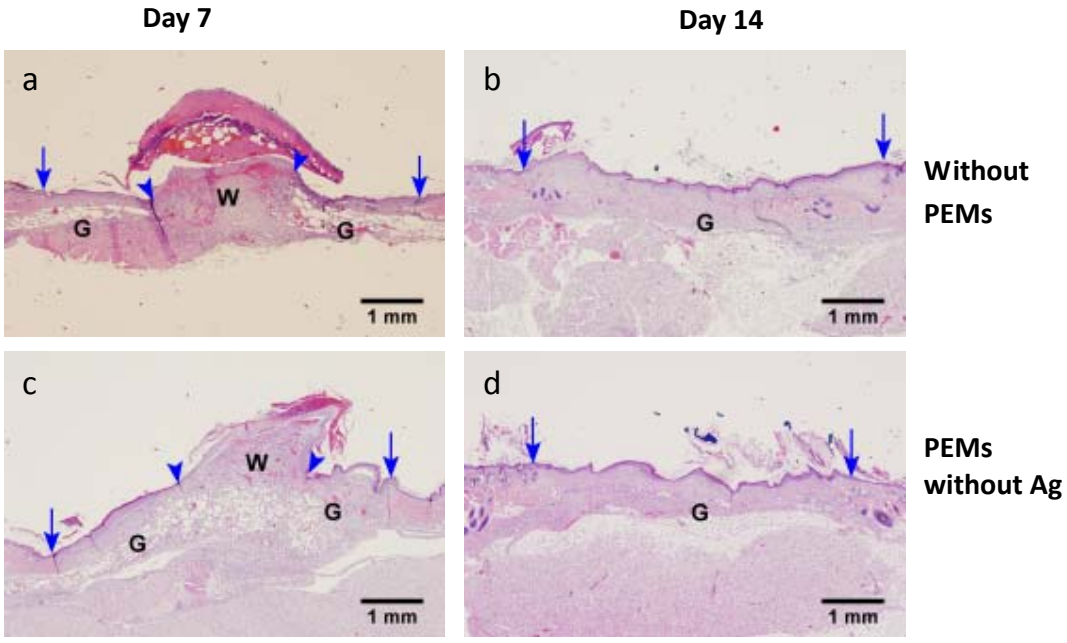

Figure S12. PEM/PVA microfilm promotes epithelialization similar to the untreated wound in excisional splinted wounds in mice, as determined by histopathology. Micrographs show H&E-stained sections post-operative days 7 and 14, respectively, of: (a, b) wounds without PEMs, and (c, d) wounds immobilized with PEMs containing no silver. Original wound edge (arrow), migrating epithelial tongue (arrow head), granulation tissue (G), and wound matrix (W) are marked.